

β -decay of very neutron-rich Rh, Pd, Ag nuclei including the r-process waiting point ^{128}Pd

F. Montes¹, T. Davinson², T. Faestermann³, H. Geissel¹, R. Gernhäuser³, M. Gorska¹, K.-L. Kratz⁴, Y. Litvinov¹, A. Musumarra⁵, C. Nociforo¹, B. Pfeiffer⁴, H. Schatz⁶, C. Scheidenberger¹, K. Sümmerer¹, H. Weick¹, P. Woods²

¹ GSI, Darmstadt, Germany

² The University of Edinburgh, Scotland

³ Technische Universität München, Germany

⁴ Institut für Kernchemie, Universität Mainz, Germany

⁵ Laboratori Nazionali del Sud, INFN Catania, Italy

⁶ NSCL, Michigan State University, USA

Motivation

The astrophysical origin of about half of the elements heavier than iron existing in the universe has been attributed to the rapid (r-) neutron capture process. In addition to astronomic observation studies of the r-process abundance pattern in the solar system and in metal-poor r-process enriched stars, the r-process has motivated not only experimental but also theoretical studies of neutron-rich nuclei.

To correctly link astronomical observations with theoretical models, reliable nuclear physics input are needed. To date, about 50 nuclei along or near the r-process path have limited experimental information. Because the proposed path of the r-process in the nuclei chart runs far away from stability and despite the amount of research, the question if properties of nuclei far away from stability can be derived from properties of nuclei closer to stability is an important one and still remains unresolved. Furthermore, the origin of the r-process is still unknown and no astrophysical scenario has been identified with certainty.

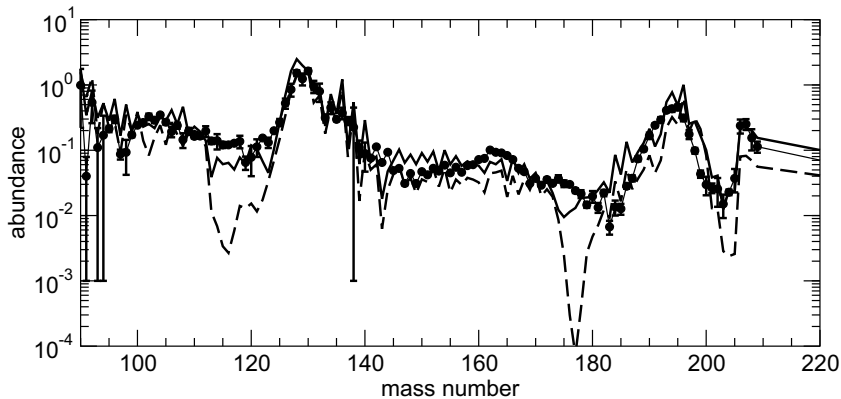


Figure 1: Solar r-process abundances (dots) and abundances predicted using a classical r-process model[1]. The solid line shows the predictions based on the ETFSI-Q mass model assuming a quenching of the neutron shell gaps far from stability. The dashed line shows the predictions based on the ETFSI-1 mass model without such shell quenching.

The region around the $N = 82$ shell closure is particularly important in r-process studies because it is responsible for the observed $A = 130$ peak in the solar system r-process abundance distribution. In addition, the region $A = 113 - 124$ is very sensitive to the nuclear structure properties as shown in Fig. 1. Nuclear structure

effects linked with shell quenching are believed to explain the underabundance observed when comparing r-process calculations with the solar r-process abundance in this region[2]. In addition, neutrino spallation reactions may also affect abundances in this region[3] and there are also indications that a second r-process is needed to explain the solar abundances of some nuclei in the $A = 90 - 130$ mass region based on observations of the abundance pattern in r-process-enhanced extremely metal-poor stars [4, 5]. In order to disentangle the various neutron capture processes potentially contributing to the origin of the $A = 90 - 130$ nuclei in nature, solid nuclear data is required.

The most important nuclear data inputs necessary to successfully model the r-process are β -decay half-lives ($T_{1/2}$) of the participating nuclei, β -delayed neutron emission branchings (P_n) and nuclear masses. Because of the relatively long half-lives of nuclei participating in the r-process path when it reaches the $N = 82$ shell closure, these isotopes serve as bottlenecks where material accumulates. While the neutron separation energies determine the location of the bottlenecks, the β -decay half-lives determine how much material accumulates on them during the process. When the neutron flux is exhausted, P_n values change the final abundance composition while the material finally decays back towards stability.

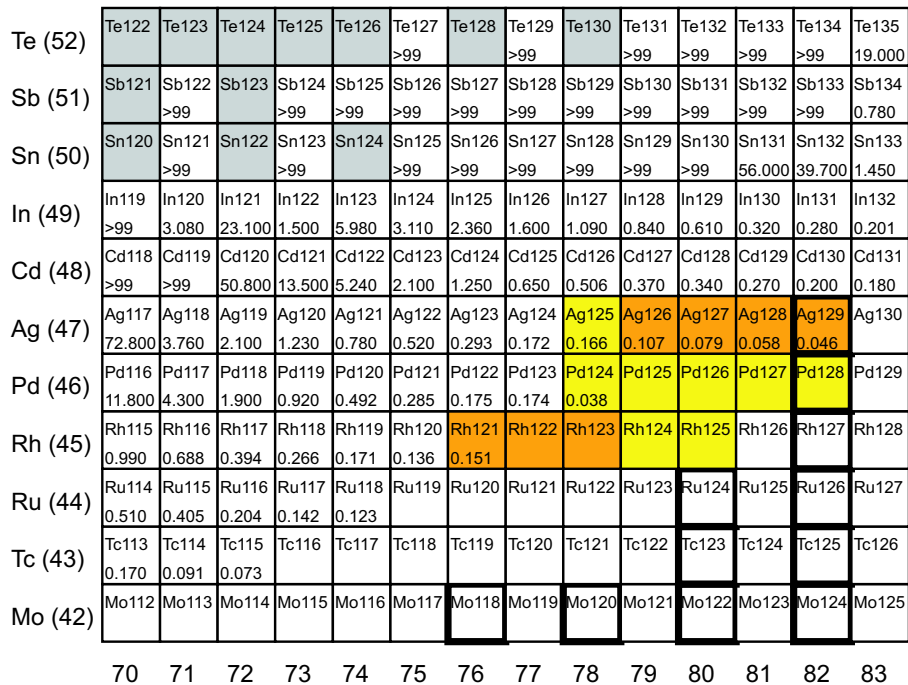


Figure 2: ^{112}Mo to ^{135}Te mass region showing the region of interest. The isotopes for which we propose to study the β decay half-lives are colored in orange and yellow. P_n values in the proposed experiment can be measured for the isotopes colored in orange. The r-process waiting points predicted with the ETFSI-Q mass model are framed with black thick lines. Stable isotopes are shaded with gray. Experimental half-lives are given in seconds below the names of the isotopes.

Figure 2 shows the proposed r-process path along the nuclear chart and the current limit of known $T_{1/2}$ in this region. Only the half-lives of ^{130}Cd and ^{129}Ag are known experimentally in the r-process path at or “bellow” the $N=82$ shell closure. The known P_n values are still too small or too far away (with the exception of ^{120}Rh) to have a direct impact on r-process calculations and no P_n value is known experimentally at the shell closure.

Properties of nuclei along the r-process path and the astrophysical conditions used in the modeling are

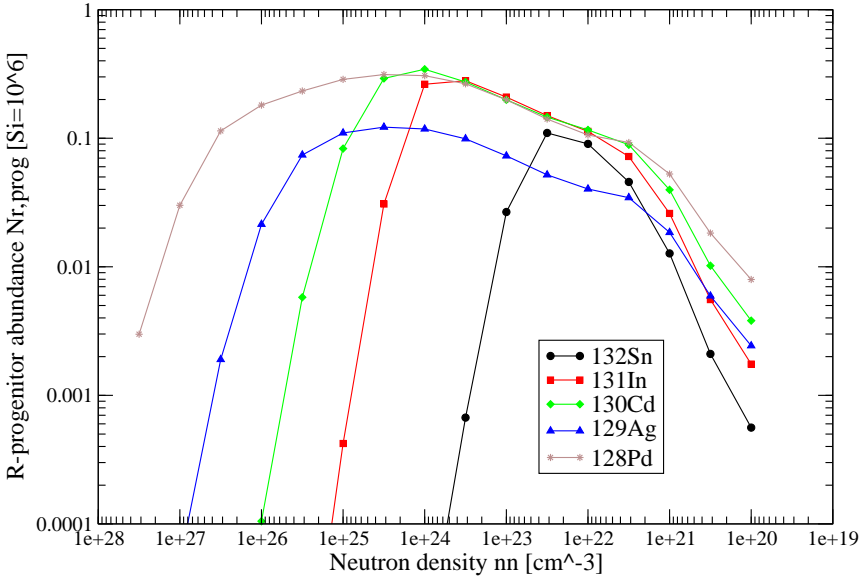


Figure 3: Calculated r-process abundances of the N=82 bottleneck isotopes as a function of neutron density. Taken from [6].

reflected in the calculated abundance pattern. Because the calculated abundances directly reproduce the observed r-process abundances, reliable nuclear input is a requisite to obtain astrophysical conditions independent from astrophysical models. Bottleneck abundances for different neutron densities at the N=82 shell closure are shown in Fig. 3. In one of the most promising r-process scenarios, the neutrino-heated wind in core-collapse supernovae, the neutron density starts around $10^{28-30} \text{ cm}^{-3}$ and eventually drops to around 10^{22} cm^{-3} when freezeout occurs. Fig. 3 can thus be seen as a progenitor abundance distribution before freezeout occurs with the time axis going from left to right. Of the progenitor bottleneck isotopes involved, only ^{128}Pd does not have any experimental information available. Moreover, because ^{128}Pd is a bottleneck of the r-process, its decay has implications in the predictions of the Th, U cosmochronometers in ultra-metal poor stars.

We therefore propose the measurement of β -decay half-lives and P_n values for the very neutron-rich Rh-Pd-Ag isotopes shown in Fig.2. While the half-lives of $^{125-128}\text{Pd}$ and $^{122-125}\text{Rh}$ will be measured for the first time, the statistical uncertainty of the known ^{121}Rh and ^{124}Pd half-lives will be greatly reduced. All the proposed P_n values are currently unknown. Expected half-lives range from milliseconds to seconds while expected P_n values are expected from 2 to 25%. Besides the direct influence of the P_n values and the ^{128}Pd half-life in r-process calculations, the remaining half-lives can be used as gross estimates of nuclear structure. Comparison of theoretical predictions with measured half-lives and P_n values will give indication of the strength of the shell closure at N=82.

Fig. 4(a) and Fig. 4(b) show existing experimental information along with theoretical estimates of the desired isotopes. Theoretical predictions are based on the quasi-particle random-phase approximation (QRPA)[7] coupled with the FRDM[8] and ETFSIQ[9] mass models. These measurements will provide direct input in r-process model and will solve discrepancies between theoretical models crucial to our understanding of the abundance pattern in this mass region.

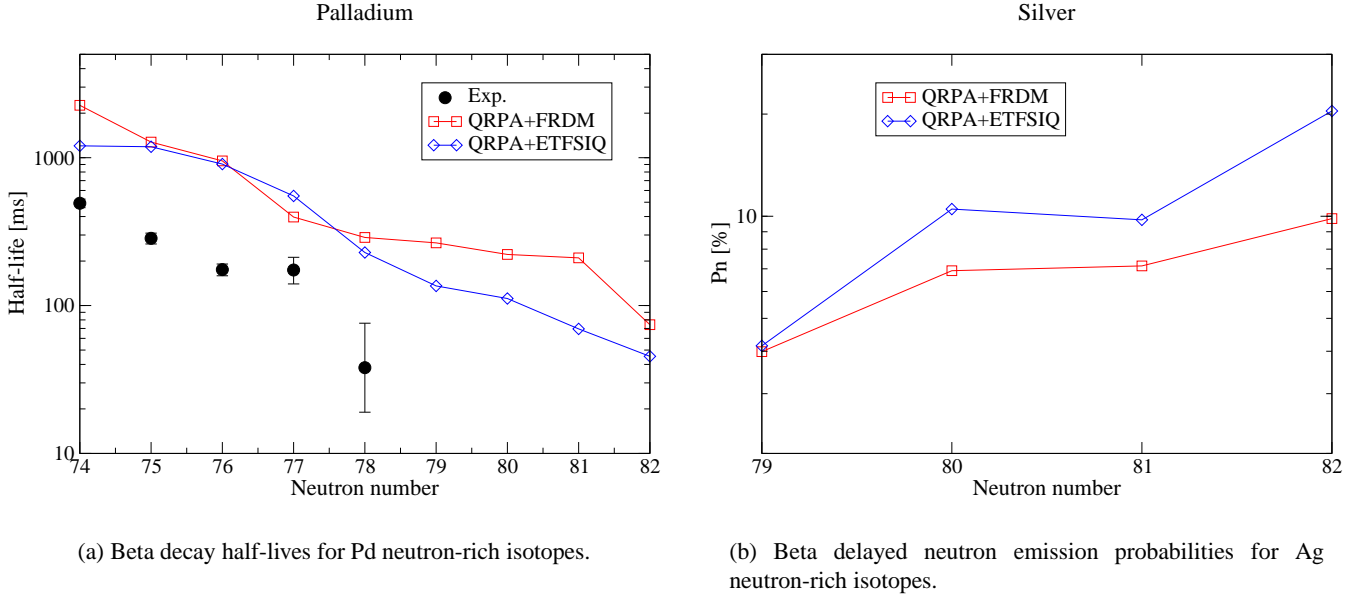


Figure 4: Experimental data is shown when available. Theoretical predictions are based on the quasi-particle random-phase approximation (QRPA)[7] coupled with the FRDM[8] and ETFSIQ[9] mass models.

Experimental details

In the proposed experiment neutron rich nuclei are produced in two steps. First, a beam of ^{132}Sn is produced by fission of ^{238}U accelerated to 1 A GeV impinging onto a 2400 mg/cm^2 Pb target and then transmitted to the intermediate image plane (F2) of the FRS. Secondly, the specific neutron-rich isotopes are produced by fragmentation of the ^{132}Sn beam in a 5500 Be mg/cm^2 target located in F2. The reaction products after fragmentation are separated according to mass and charge in the second part of the FRS and unambiguously identified. Magnetic rigidity, time-of-flight, energy loss and position of each fragment is measured event-by-event using the standard set of detectors at the F2 and F4 planes at the FRS.

A similar two-step reaction scheme has been discussed before in [10] and it is predicted to give the highest rates for the particles of interest than by pure fragmentation or fission reactions. Cross sections for the fission process were taken from the results of a previous GSI experiment[11]. Fragmentation cross sections were taken from theoretical estimates using EPAX[12] and ABRABLA/COFRA[13]. Accepted experiment E294[14] plans to measure fragmentation cross sections of neutron-rich nuclei and in particular the ones of interest.

Once the neutron-rich nuclei are transmitted to F4, they are slowed down in a variable degrader and stopped in an implantation detector at F4. An overview of the proposed setup is shown in Fig. 5. The implantation detector consists of a stack of segmented silicon detectors where each implantation is detected and recorded along with its position and time. β particles are detected in Si detectors and spatially correlated with implantations. β decay half-lives will be determined by detecting the time difference between implantation and decay. In addition, a neutron detector will be used to measure neutrons emitted in coincidence with a β decay. P_n values are extracted using a ratio between $\beta - n$ coincidences and β decays for a specific isotope. The neutron detector consists of 3 concentric rings of ^3He proportional gas counters embedded in a polyethylene moderator matrix. Expected neutron energies are in the range of hundreds of keV where the neutron detector

efficiency is roughly 30%.

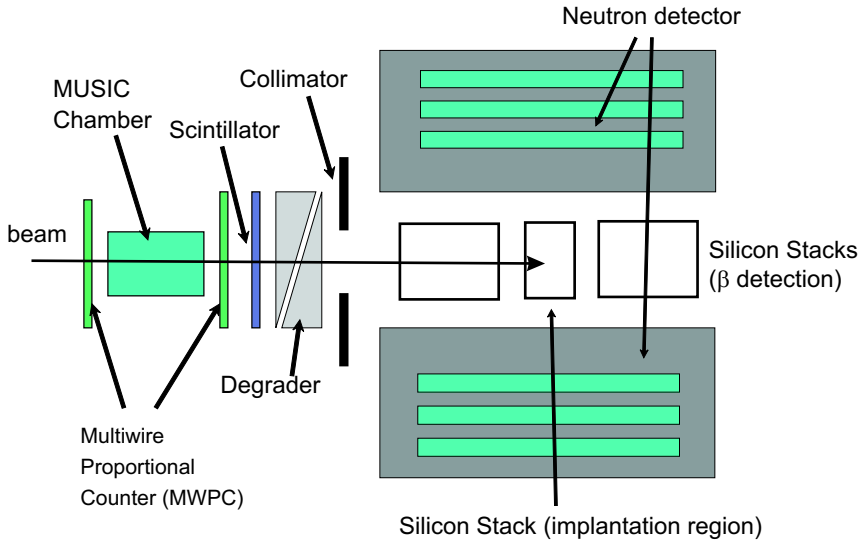


Figure 5: Schematic Diagram of the experimental setup at the FRS focal plane F4.

Beam time request

Table 2 shows expected implantation rates, total number of detected β particles and total number of detected β -neutron coincidence events. These numbers are based on an incident ^{238}U beam intensity of 2×10^9 ions/spill and a lead target of 2400 mg/cm^2 . Particle identification of the secondary beam ^{132}Sn and optimization of the transmission to F2 will be done at the beginning of the experiment and we expect a rate of around 10^4 ^{132}Sn ions at F2 assuming a transmission of 8% calculated with the program MOCADI. Two different settings centered at ^{125}Pd and ^{128}Pd in the second part of the FRS will be used. Changing the Be reaction target thicknesses from 5500 to 5000 mg/cm^2 but keeping the magnetic settings constant will allow the addition of statistics without a change in the particle identification. To account for the difference between theoretical fragmentation cross section predictions from EPAX and COFRA codes, the estimated production rate was divided by a factor of 10.

Because F4 will effectively work as a dispersive plane for the reaction fragments, transmission and implantation efficiencies for different isotopes vary widely. Total implantation rates are calculated to be less than 10 ions/s to prevent multiple implantations in the same pixel of the Si detector before the β -decay takes place and to avoid background from accumulated activity in the detector. The accuracy of the measurements depends on statistics and for the case of half-lives, it will range from 5% to 15%. For P_n values, the accuracy will vary from 10% to 25%.

Based on the intensity estimates we request 27 shifts of beam time and 6 shifts of parasitic ^{136}Xe beam to calibrate the FRS and detectors before the main beam time.

References

- [1] K.-L. Kratz et al. Ap. J. **403**, 216 (1993).
- [2] B. Pfeiffer et al., Nucl. Phys. A **693**, 282 (2001).

Table 1: Calculated implantation rates, detected β particles, and detected β -neutron coincidence events (β -n events) for the nuclei of interest for the different FRS fragment settings. The EPAX code was used to estimate the production cross sections of the various isotopes in the Be target. The implantation rates have been divided by 10 to account for a possible over-prediction of production cross sections. Predicted P_n values are taken from the QRPA calculations in Ref. [2] and Ref. [15].

Isotope	Rate (10^{-3} s^{-1})	Detected β particles	Detected β -n events	$P_n(\%)$
Central Fragment: ^{128}Pd 12 shifts				
^{129}Ag	2.7	282	17	13.1
^{128}Ag	1.4	145	4	4.9
^{128}Pd	0.4	34	2	7.6
^{127}Pd	0.8	86	2	3.9
^{126}Pd	1.2	122	2	1.5
^{125}Pd	0.8	75	1	1.5
^{126}Rh	0.1	7	1	29.4
^{125}Rh	0.3	25	2	16.9
^{124}Rh	0.5	55	3	11.2
^{123}Rh	0.8	74	5	12.5
^{122}Rh	0.5	46	3	10.5
Central Fragment: ^{125}Pd 15 shifts				
^{129}Ag	3.5	394	24	13.1
^{128}Ag	9.0	1166	26	4.9
^{127}Ag	16.1	2084	44	4.6
^{126}Ag	15.5	2011	39	4.3
^{127}Pd	0.3	36	1	3.9
^{126}Pd	1.4	177	3	2.9
^{125}Pd	4.1	529	4	1.5
^{124}Pd	6.7	861	2	0.4
^{124}Rh	0.2	27	2	11.2
^{123}Rh	0.9	114	7	12.5
^{122}Rh	2.4	304	15	10.5
^{121}Rh	3.4	435	13	6.6

Table 2: Beam time request

Parasitic beam time	
projectile	beam time
^{136}Xe (1 A GeV)	2 days

Main beam time			
projectile	1^{st} FRS section	2^{nd} FRS section	beam time
^{238}U (1 A GeV)	FRS calibrations		1 day
^{238}U (1 A GeV)	^{132}Sn	^{125}Pd	5 days
^{238}U (1 A GeV)	^{132}Sn	^{128}Pd	4 days

Total requested beam time	
main beam time ^{238}U	10 days
parasitic beam time ^{136}Xe	2 days

- [3] M. Terasawa et al., *Astrophys. J.* **608**, 470 (2004).
- [4] J.J. Cowan et al., *Astrophys. J.* **572**, 861 (2002).
- [5] C. Sneden et al., *Astrophys. J.* **591**, 936 (2002).
- [6] A. Wöhr et al., Beta decay studies of r-process nuclides in the ^{132}Sn region, Third Int. Conf. on Fission and Properties of Neutron-Rich Nuclei, Nov. 3, 2002, Sanibel Island, Florida.
- [7] P. Möller et al., *Nucl. Phys. A* **514**, 1 (1990).
- [8] P. Möller et al., *At. Data Nucl. Data Tables* **59**, 185 (1995).
- [9] J.M. Pearson et al., *Phys. Lett. B* **387**, 455 (1996).
- [10] K. Helariutta et al., *Eur. Phys. J. A* **17**, 181 (2003).
- [11] J. Benlliure, private communication.
- [12] K. Sümmerer and B. Blank, *Phys. Rev. C* **61**, 034607 (2001).
- [13] J. Benlliure et al., *Nucl. Phys. A* **660**, 87 (1990).
- [14] J. Benlliure et al., Fragmentation of very neutron-rich projectiles around ^{132}Sn , Proposal S294 GSI, (2004).
- [15] P. Möller, J. R. Nix, and K.-L. Kratz. *At. Data Nucl. Data Tables* **66**, 131 (1997).